Laser and Particle Beams (2001), *19*, 393–402. Printed in the USA.

Study of imploding plasmas at the Kurchatov Institute

YU. KALININ, A. KINGSEP, L. RUDAKOV, AND K. CHUKBAR
Russian Research Center "Kurchatov Institute," 123182, Moscow, Russia
(RECEIVED 22 May 2000; ACCEPTED 20 April 2001)

Abstract

The goal of the experiments on "Module A-5" and S-300 machines for some 15 years was to study the "liner-converter" inertial confinement fusion (ICF) scheme. A new class of fast instabilities of *z* pinches was studied both in experiments and in analytical theory. Stabilization of the light liner has been achieved by means of an extrinsic magnetic field. Formation of thin overheated current-carrying shells has been predicted analytically and seems to be really observed. Both theory and simulations predict growing T_e and heat flux onto the converter by using heterogeneous *z* pinches with spatially separated regions of efficient energy exchange and of efficient heat conductivity. In our first experiments of this kind, impurities were inserted by means of placing thin glass fibers into a He jet. Growing intensity of the spectral lines of He-like chlorine from the cathode surface confirms the growth of heat flux. Theoretical investigations and 2.5-D simulations were devoted to some basic points of this program.

1. INTRODUCTION

The last decade has seen enormous progress in pulse-power techniques to produce X rays by means of the hot, dense *z* pinches. The multiwire array approach to creating high atomic number plasmas offers a highly efficient conversion of magnetic energy into soft X-ray (SXR) blackbody radiation. Nowadays, Sandia National Laboratories' Z accelerator achieves a peak power of X-ray emission as high as 280 TW from a macroscopically stable 2-cm-long tungsten-plasma *z* pinch resulting in 1.8 MJ blackbody radiation (Quintenz *et al.*, 2000).

Some other experimental programs were based on slightly different ideas. In particular, a "liner-converter" program was developed at the Russian Research Center's "Kurchatov Institute" (Rudakov *et al.*, 1991). The basic ideas of this approach are the following:

1. The transformation of a significant fraction of the kinetic energy of a light liner, via an implosion, while providing an efficient thermal isolation of the liner "walls," into the heat of relatively dilute plasma fill.
2. The transport of this heat onto an edge converter *via* electron heat conductivity. Sharpening the pulse has to be brought about by the "thermal gate" conditioned by the nonlinear dependence of the electron heat conductivity with temperature, $q \propto T_e^{3/2}$. Then, this energy will be radiated by the converter in the X-ray range.

Such a scheme, because of the effective separation of the energy accumulator and radiator, allows one to vary the output spectrum of the X rays, depending upon the material of the converter, from several hundred electron volts (Pb, W) up to several dozen kiloelectron volts (Kr, Mo). Thus, not only the soft X-ray radiation but also the hard X-ray radiation (HXR) range (10–30 keV) becomes available. From this standpoint, the liner-converter scheme may compete with the "liner–liner impact" scheme (Rudakov *et al.*, 1997). Low-density plasma fills (H, He) may be heated efficiently due to low radiation heat losses, whereas fast heat transport onto the converter is conducive to the efficient subsequent radiation of *K* lines of the converter material.

One of the main problems of the liner-converter scheme comes from its multistage organization; another turns out to be the straightforward consequence of the nonlinearity mentioned above. As a result, the radiation output from the converter should obey essentially nonlinear dependence on the current. It becomes noticeable (and the scenario may be realized) only if $I > 10$ MA. We cannot operate with such a current value at the present generation of our machines; therefore we concentrated our efforts on solving some important particular problems of the liner-converter approach:

1. Instabilities of light liners and their stabilization.
2. Enhanced efficiency of ion–electron energy exchange during implosion.

Address correspondence and reprint requests to: Yu. Kalinin, Russian Research Center, "Kurchatov Institute" 123182, Moscow, Russia. E-mail: vikhrev@nfi.kiae.ru

3. Experimental realization of the whole scenario at the current level of power engineering and comparison of its results with simulations.

2. EXPERIMENTAL SETUP AND DIAGNOSTICS

Our experiments were based on "Module A-5" (Bol'shakov *et al.*, 1982) and S-300 (Bakshaev *et al.*, 1997) machines; a fraction of the experiments were carried out on the French generator "AMBIORIX" (Gasque *et al.*, 1998).

The generator Module A-5 ($V = 2$ MV, $I \sim 0.8$ MA, $\tau \sim$ 140 ns, output impedance $\mathbf{Z} = 2.2\ \Omega$) was constructed as a high-current accelerator. To couple it to the liner or *z*-pinch load, a special pulse transformer was constructed based on 48, water-insulated transmission lines (Baranchikov *et al.*, 1978). It provided a transformation coefficient $K = 6$ with an output impedance $\mathbf{Z} = 0.04\ \Omega$. As a result, peak currents up to 2.2 MA in a liner were achieved. We will not describe Module A-5 in detail since this installation was mentioned and described many times; hereafter we will dwell on the brief description of the S-300 machine.

The S-300 generator ($V = 1.3$ MV, $P = 10$ TW, $\tau = 45$ ns) was constructed on the basis of well-known multimodule principles (eight modules) and consists of a capacitive-energy storage system, two water stages of pulse-forming, water transmission lines, and a vacuum chamber with energy concentrator inside it. The output pulse-forming stages, the transmission lines, and the vacuum chamber were situated within the common tank (Fig. 1).

The capacitive-energy storage system consists of eight, vertically-arranged Marx generators placed around the central tank within the 9-m-diameter area and situated in separate tanks filled with transformer oil. They charge the first water stage of the pulse-forming system. The Marx housings are made of epoxy compounds strengthened with fiberglass material. Each Marx generator stores 115 kJ and consists of 20 stages charged up to ± 85 kV and switched by three-electrode triggered gas switches (nitrogen up to 0.4 MPa). In addition, the first four switches are mounted in a unibody case with ultraviolet spark gap light illumination for switch triggering improvement.

The first stage of water pulse-forming consists of eight, water-filled intermediate storage (IS) capacitors and it serves to rapidly charge the output pulse-forming stage. The IS system itself may be charged up to 3.5 MV for 1.3 μs. Each IS is a cylindrical, water-insulated 15-nF capacitor that is

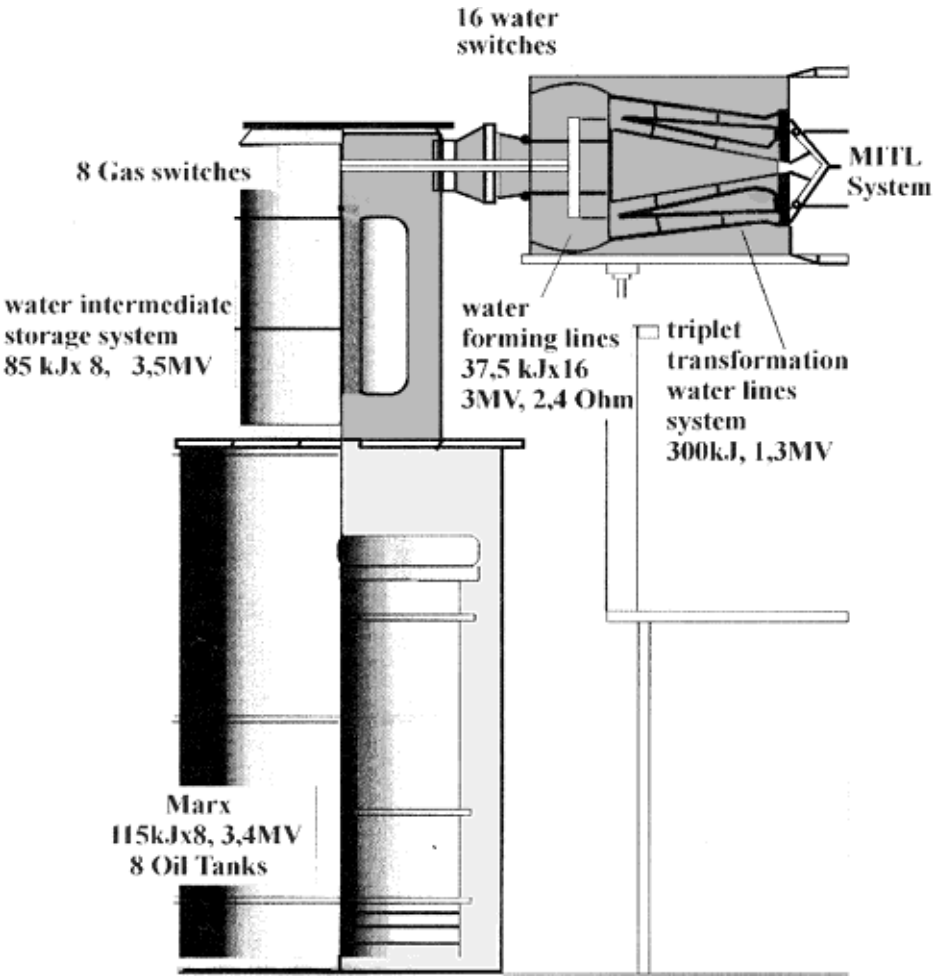

Fig. 1. S-300 generator.

https://doi.org/10.1017/S0263034601193110 Published online by Cambridge University Press

mounted vertically on the corresponding Marx generator and is switched by an actively triggered four-electrode gas (SF_6) switch installed in the upper part of the IS. The Marx (oil) and IS (water) volumes are separated by an insulator made of an epoxy-polyurethane compound.

The output pulse-forming stage is a system of pulse forming lines (PFLs) consisting of 16 planar water lines with a wave impedance of 4.8 Ω each and electric length of 30 ns, charged up to 3.2 MV for 180 ns and switched by a system of self-breaking multichannel water switches. Each water line has seven pairs of switch pins. A special feature of the PFLs is that the switching occurs in the middle of each line. The technique decreases by a factor of two its wave impedance and the forming pulse length. The total output wave impedance of the PFL system is $\mathbf{Z} = 0.15\ \Omega$.

Thus formed, the electromagnetic pulse in the planar, tri-plate water lines is transmitted into a high-voltage vacuum chamber. The latter is assembled out of four insulator rings with an inner diameter of 100 cm and 20-cm high, made of an epoxy-polyurethane compound and vacuum sealed to the electrodes. The dielectric insulator ring's geometry and that of the surrounding electrodes was selected according to the calculated electric field value on the dielectric-vacuum surface. The tangential electric field strength, E_τ, for the highest operation voltage is less than 70 kV/cm and near the "triple point" it does not exceed 50 kV/cm. The energy concentration in the liner load is accomplished by means of a three-dimensional vacuum concentrator made of 16 parallel tri-plate magnetically insulated transmission lines which are united in a liner unit. The total inductance of the vacuum chamber together with that of the energy concentrator is 10 nH. In the operating regime, S-300 provides a current of 4.2 MA into a short circuit and up to 3.6 MA into a liner load.

In combination with diagnostics that recorded the electrical parameters of the power pulse, we used the following basic diagnostics: (i) photographs in visible light region, both with streak and with framing image-converter cameras; (ii) photographs in the region of soft X rays and VUV radiation with framing image-converter cameras; (iii) recording of the radiation pulses by a set of vacuum and semiconductor X-ray diodes shielded with various filters; and (iv) convex-mica crystal X-ray spectrograph with a two-dimensional spatial resolution. In addition, a series of laser diagnostics was used in our experiments. The first method included three-frame shadow or Schlieren photography of light liners and *z* pinches using the second harmonic of Nd:YAG laser radiation. The second method was intended to determine the initial density distribution in the gaseous liner. There exists a problem of measuring the initial density of various gas jets in light (20–200 μg/cm for a diameter of several centimeters) gas puffs. This problem was solved by photographing the radiation beam of the XeCl laser in the Rayleigh-scattered light. A typical experimental setup is presented in Figure 2.

3. EXPERIMENTS WITH THE GAS-PUFF LINERS

A vast series of experiments with imploding gas-puff liners was carried out on both Module A-5 and S-300 machines

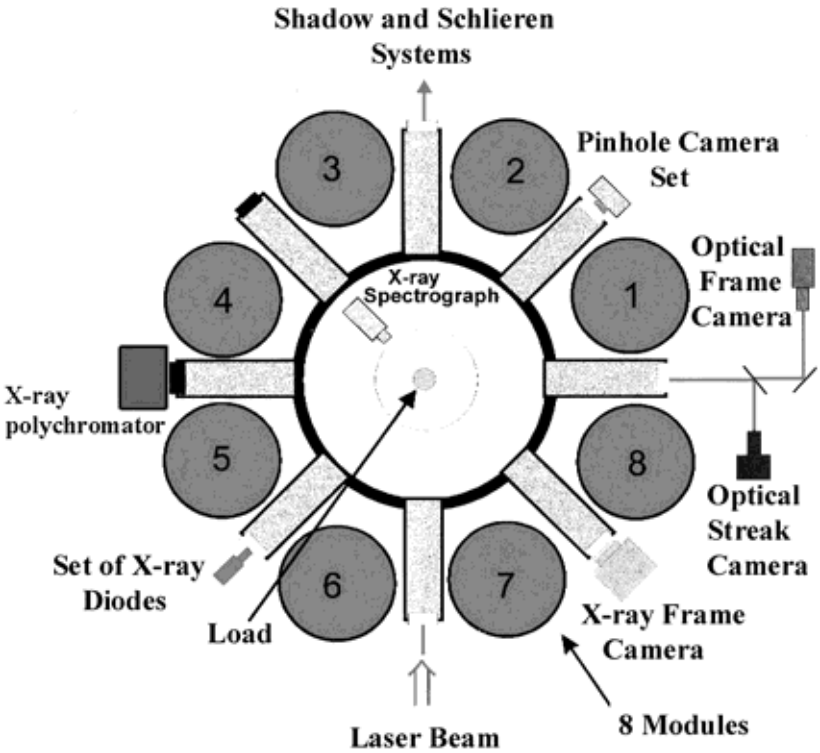

Fig. 2. S-300, layout of the diagnostics.

https://doi.org/10.1017/S0263034601193110 Published online by Cambridge University Press

(Bogolyubsky *et al.*, 1988; Chernenko *et al.*, 1996). For a load, a supersonic gas jet was used, created with a ring-like nozzle with typical Mach number of 3–5 combined with the fast-operating pulse valve (explosive or electromagnetic). In various experiments we were using N_2, He, D_2, SF_6, Ar, and Ne and their mixtures. The initial gas density could be varied over a wide range of values by varying the time delay between the opening of the valve and the application of high voltage.

One of the most important features of the implosion of efficiently radiating gaseous shells (i.e., $Z \gg 2$) was the delay time of the implosion compared to both 0-D and 1-D simulations. In addition, their final velocity and kinetic energy turned out to be less than those following from the electrical measurements and conservation laws. Some dozen nanoseconds before the inner boundary of hollow *z* pinch reached the axis, a luminous forerunner (a thin *z* pinch) appears near the axis. It is important to note that in most cases, this boundary is moving with almost constant velocity. Normally, VUV and SXR radiation appear 50–100 ns earlier with respect to the inner boundary convergence (Fig. 3). All these facts taken together are seen as the manifestation of *z*-pinch instability. Such an idea is supported by the photographs of the imploding liner in visible light and SXR with framing image-converter cameras as well as by the laser shadow photographs. To wit, starting from 80–130 ns after the current front, a striation-like modulation of the brightness appears (see Fig. 3) with a spatial period ~0.8–2.0 mm depending on the chemical composition of the jet. A forerunner on the axis appears simultaneously; its radiation is a soft one ($h\nu < 100$ eV). It is interesting to note that at this moment of time, the outer boundary usually passes the way at less than the initial thickness of the gas jet. At first glance, this excludes, *a priori*, the Rayleigh–Taylor instability. As our experiments show, the whole scenario of the current-carrying shell evolution turns out to be too complicated to use such primitive estimates.

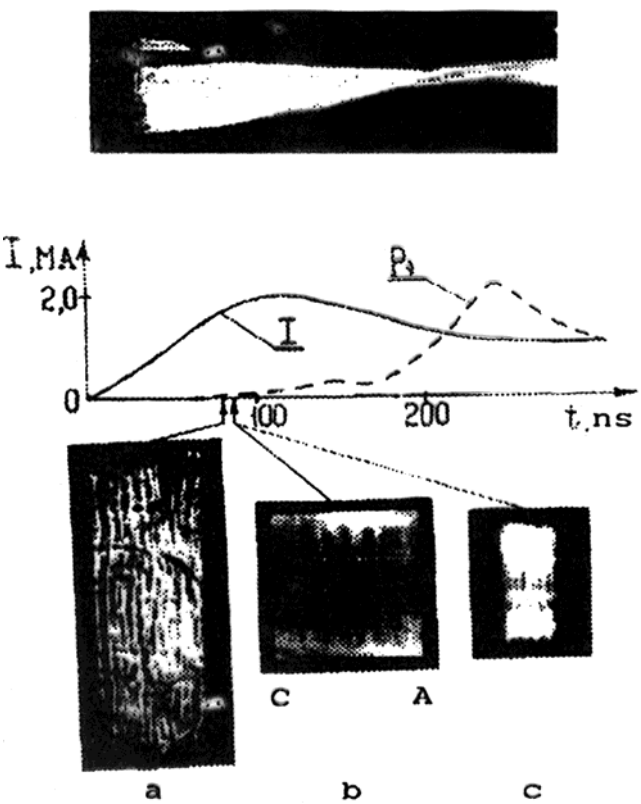

Fig. 3. Dynamics of implosion of a gaseous (N_2) liner. Top: scenario; bottom: (a) shadow photograph, (b, c) frame pictures in soft X-ray and visible range, respectively.

Let us discuss the results of the laser probing with simultaneous taking shadow and Schlieren pictures in the light of second harmonics of the Nd:YAG laser ($\lambda = 0.532$ μm) (see Fig. 4). The laser pulse duration was 7 ns, the energy radiated in the second harmonic is 20 mJ. The aperture of the recording system was as large as possible for our conditions, to wit, 0.25. The smallest gradient of electron density that might be resolved owing to the refraction in the shadow channel had to satisfy the following condition: $\nabla N_e > 2 \times 10^{21}$ cm^{-4}; in our case, it corresponds to $N_e > 2 \times 10^{20}$ cm^{-3}. For an N_2 initial gas jet, with $T_e \sim 10$ eV, the minimal ion density should be about $5–7 \times 10^{19}$ cm^{-3}.

In the Schlieren channel, the filament was placed in the focus of the lens, parallel to the *z*-pinch axis; thereby only the components of electron density gradients normal to the axis were recorded. In Figure 5, results of laser probing at a time 80 ns after the start of current are presented. It is obvious from the Schlieren photograph, that the outer boundary of the liner has moved only 3–4 mm at this moment, and

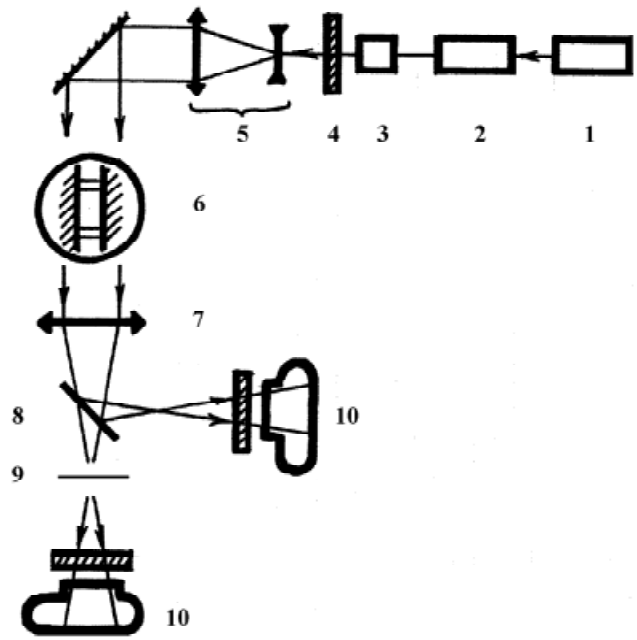

Fig. 4. Principle scheme of simultaneous shadow and Schlieren photography. 1,2: optical generator and amplifier, respectively, 3: nonlinear crystal, 4: optical filter, 5: telescope, 6: liner, 7: lens, 8: separating plate, 9: Schlieren filament, 10: cameras with filters.

https://doi.org/10.1017/S0263034601193110 Published online by Cambridge University Press

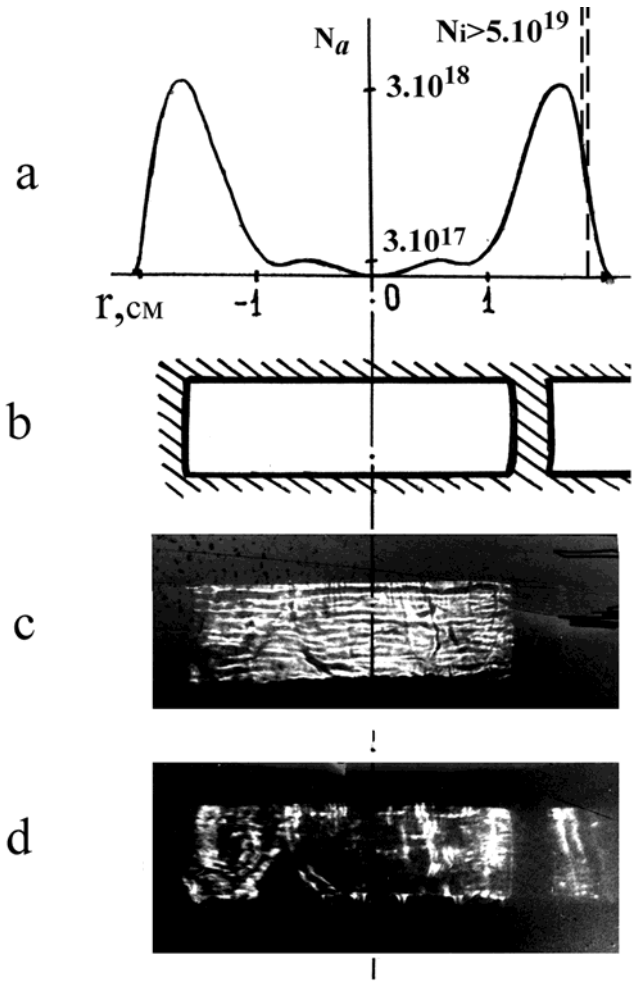

Fig. 5. Results of the laser probing of a gaseous (N_2) liner: (a) initial distribution of the gas density (solid curve); dotted line shows a model distribution of ions on the liner boundary that is necessary to provide the absorption observed; (b) geometry of the return current conductor with a diagnostic window; (c) shadow photograph of a liner at 80 ns after the start of the current; (d) Schlieren photograph at the same moment of time; the Schlieren filament was parallel to the liner axis.

only some 5×10^{18} ions have been involved in the acceleration process. On the shadow photograph, one can see the narrow ($\sim$0.01 cm) transparent "striations" perpendicular to the liner axis. The typical distance between them is of order 0.1 cm, and the contrast $I_{max}/I_{min} \sim 5$. Let us emphasize that the effect of a shadow by so small a mass value and with a fairly big radii ($R \approx 1.6$ cm) should be seen as evidence of the formation of a very thin and dense shell. To provide the absorption *via* inverse Bremsstrahlung, its thickness cannot exceed 2×10^{-2} cm by $N_i \geq 2 \times 10^{19}$ cm^{-3}. If, in addition, the approximate equilibrium between radiation and Ohmic heating takes place, which corresponds to $T \sim 10$ eV, the following equality is satisfied inside the shell:

$$B^2/8\pi = (N_i + N_e)T.$$

Thus, we seem to give the first experimental demonstration of the "snow-plough" regime.

The estimated thickness of the shell turns out to be basically less than the skin depth, $\delta = \delta_{sk} = \sqrt{c^2\tau/4\pi\sigma} \approx 0.1$ cm. As a result, a breakdown on the inner boundary of the liner may occur, resulting in the formation of precursors on the axis. Such a scenario was first considered in Chukbar (1993; see also below). In principle, formation of such a thin shell may result in the small-scale Rayleigh–Taylor instability. However, just in our case, the reason for striations seems to be different. The following conclusions were made on the base of numerous experiments (Bogolyubsky *et al.*, 1988; Rudakov, 1989; Chernenko *et al.*, 1996):

1. If we compare the dynamics of implosion of liners with equal masses but different composition, it turns out that the liner with lower atomic numbers is more stable. On the other hand, more massive shells are more stable compared to lighter ones, in particular, with current values $I \sim 2.5$–3 MA, hollow z pinches with $dM/dl \sim 400$–500 μg/cm remain stable during implosion.
2. Instabilities observed are being efficiently developed even during the phase of implosion corresponding to the constant velocity of the liner motion. Moreover, they manifest themselves even at the earliest stage, for example, after the displacement of the shell as small as ~ 0.1 of its initial radius.
3. The typical thickness of the shell, 2×10^{-2} cm $<$ c/ω_{pi}, is so small that the conventional MHD approach resulting in the Rayleigh–Taylor instability may not be used. Instead, one must deal with electron magnetohydrodynamics (EMHD; Kingsep *et al.*, 1990).

The theory of the fast EMHD instability of hollow imploding z pinches was presented in Rudakov *et al.* (1989) and Rudakov and Sevastianov (1996). One of its important consequences is the following: such an instability may be suppressed by the shear of magnetic field lines that can be provided by a respectively small B_z field. This longitudinal magnetic field is necessary also to prevent heating of the liner walls instead of the edge converter. Indeed, the ratio of the total heat flux onto the converter to that onto the liner walls is, roughly speaking, $(R_f/l)^2$ where R_f is the final pinch radius and l is its length. In our experiments, we succeeded in stabilizing the process of liner implosion by applying the longitudinal magnetic field $B_z \sim 5$–10 kG. As a result, the whole physical modeling of the liner-converter scheme was brought about in our experiments on the Module A-5 (Rudakov *et al.*, 1990, 1991) and AMBIORIX (Gasque *et al.*, 1998; Zehnter *et al.*, 1998) machines. As an example, let us describe our experiment on the Module A-5. Its scheme is presented in Figure 6. A thin mica plate situated near the cathode, 45° to the pinch axis, played the role of a converter. As basic diagnostics, we used simultaneous image converter photographs in two different spectral inter-

https://doi.org/10.1017/S0263034601193110 Published online by Cambridge University Press

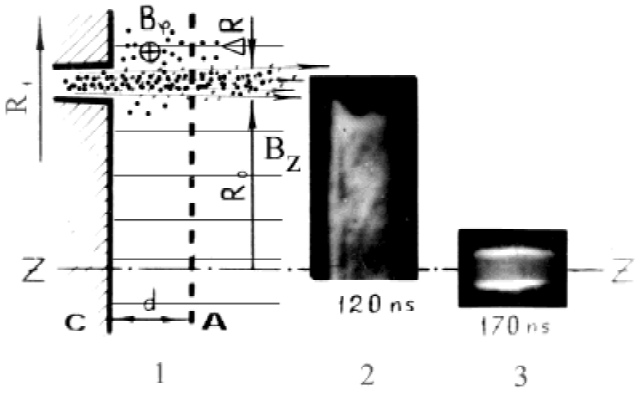

Fig. 6. Liner implosion with a longitudinal magnetic field: (1) scheme of the experiment, (2) liner photograph in soft X-rays at the moment of maximal current value, (3) the same at the moment of maximal compression. One can see striations inclined 45° to the axis in picture 2; in the inverted extrinsic magnetic field they change their direction by 90°.

vals of SXR: (1) 150 eV $\leq h\nu \leq$ 300 eV, and (2) $h\nu >$ 1 keV. Each ICT was supplied by the double pinhole chamber with two different filters. Experimental results are presented in Figure 7. One readily can see both the column of hot plasma and bright SXR flare in the region close to the converter where the plasma cloud is fairly cool. It is important that there is no such flare either 10 ns before the maximal compression or 10 ns after it.

4. CURRENT-CARRYING SHELL OF A STRONGLY EMITTING LINER

The self-similar model presented in this item was first formulated by Chukbar (1993) on the basis of a series of papers by Sasorov (1991) and Neudachin and Sasorov (1991). It may be applied to both liners and solid *z* pinches. The presence of the small parameter Δ/R in the former, where Δ is the liner thickness and R is its radius, causes MHD equilibrium to be established rapidly in the plasma shell. As a result, the subsequent acceleration occurs compactly. In *z* pinches, this compactness is not essential. We assume our *z* pinch (hollow or solid) to be strongly radiating because of the ion charge number $Z_i \sim 1$:

$$\frac{j^2}{\sigma}\, t \sim Q_{rad}\, t \sim nT, \tag{1}$$

where t is the characteristic time of the motion, n is the electron density, and T is the electron temperature. Using the Maxwell equation $j \sim cB/4\pi\delta$ where $\delta = R$ is the thickness of the current-carrying shell, we can rewrite (1) in the following form:

$$\frac{c^2}{4\pi\sigma}\, t \sim \delta^2\, \frac{8\pi nT}{B^2}, \tag{2}$$

from which it follows immediately that either $nT = B^2$ or $\delta = \delta_{skin}$ holds. If the former is true, the liner is a fairly uniform and cold shell in which the magnetic pressure is balanced by the inertial force (such a model was constructed and studied by Grigor'ev & Zakharov, 1987). In the second case, the liner is a highly uniform hot heterogeneous structure, in which the magnetic pressure of the hot shell is transferred to the cold internal layers (with no current flow in them) through the thermal pressure. The condition $\delta = \delta_{skin}$ can hold only in the case $\nabla \times E = 0$, $E + j/\sigma = const \Rightarrow j \propto \sigma$. Hence, in such a regime the electric field does not vanish at the current-carrying layer internal boundary, so that it is very probable that some inner breakdown occurs, resulting in the formation of precursors on the pinch axis. The resistance of the current-carrying shell should be less than the resistance of the rest of the plasma: $\sigma_h \delta > \sigma_c \Delta$, where $\Delta \leq R$ is the thickness of the cold layer. However, as will be seen below, almost all the mass is concentrated in the latter.

The particular feature of the heterogeneous regime is that the thermal instability may be stabilized only by electron thermal conductivity (Sasorov, 1991; Neudachin & Sasorov, 1991); thus, we have the following system of basic equations:

$$nT \approx \frac{B^2}{8\pi};$$

$$\frac{j^2}{\sigma} \approx \left(\frac{cB}{4\pi\sigma}\right)^2 \frac{1}{\sigma} \approx Q_{rad} \approx \frac{\kappa_e T}{\delta^2}. \tag{3}$$

Using the standard values of the kinetic coefficients (Braginskii, 1963) for an unmagnetized plasma with $Z \sim 1$ and the simple interpolation formula $Z = \sqrt{T}$ (eV), which describes the equilibrium stage of ionization for materials with $Z_{nucl} \geq 20$ in the range 30–300 eV, one can find from Eqs. (3):

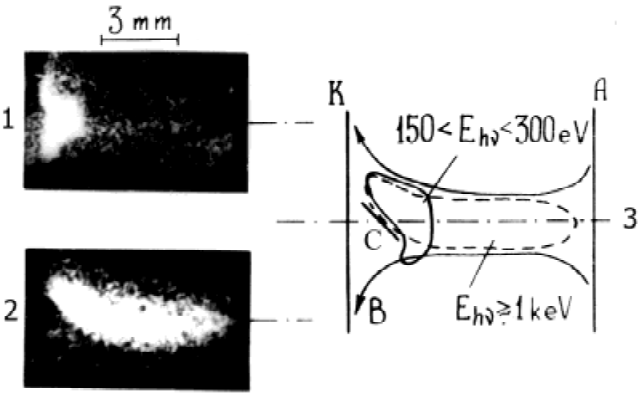

Fig. 7. Simultaneous X-ray image converter photographs of the plasma at the moment of maximal compression of the liner with an extrinsic longitudinal magnetic field: (1) 150 eV $\leq h\nu \leq$ 300 eV, (2) $h\nu >$ 1 keV, (3) schematic picture of the compressed liner: K,A: cathode and anode, respectively, B: magnetic field lines, C: mica converter.

https://doi.org/10.1017/S0263034601193110 Published online by Cambridge University Press

$$\omega_{ce}\tau_e \cong 1, \qquad T \approx 100\sqrt{B}, \qquad n \approx 2 \times 10^{20} B^{3/2}. \qquad (4)$$

Here ω_{ce} is the electron cyclotron frequency, $\tau_e = T^2/(nZe^4\nu_{Te}\Lambda)$ is the Coulomb relaxation time, T, n, and B are expressed, respectively, in units of eV, cm^{-3}, and MG. The very important thing is that all of the relations in (4) are almost insensitive to the variation of the material.

Let us take as an example the Xe liner by $B = 1$ MG; hence, $n \approx 2 \times 10^{20}$ cm^{-3}, $T = 100$ eV. Under such conditions, $Z \sim 10$ the coronal radiation regime (Post *et al.*, 1977) xenon has $Q_{rad} \sim 10^{-17}\, n^2/Z$ (ergs/s); thus we obtain from (3) $\delta \approx 10^{-4}$ cm. For a Xe liner with $I = 2.5$ MA and $R = 0.5$ cm, the mass per unit length turns out to be equal to 1.5 μg/cm. In particular, that means only a very small fraction of the mass is being contained in the current sheath.

For the light materials, for example, H and He, bremsstrahlung is the dominating mechanism of radiation losses. For such a case, it may be proved that such a regime of overheating hardly can be realized. For instance, for hydrogen, $dm/dl \approx 0.3RB^{3/5}$ mg/cm where R is given in centimeters.

Except for the inner breakdown, small-scale Rayleigh–Taylor instability may join the game. As a whole, the problem of overheating seems to be one of disadvantages of the gas-puff *z* pinch of heavy materials, compared to wire arrays.

5. NUMERICAL SIMULATION OF THE PLASMA COMPRESSION BY A LIGHT LINER

Our numerical study of liner implosion and compression of plasma filling have been presented (e.g., in Gasque *et al.*, 1998; Kosarev *et al.*, 1989; Kingsep *et al.*, 1997). In this article, we restrict ourselves to some examples of modeling Rayleigh–Taylor instability.

The dynamics was considered on the basis of 2-D *r–z*, one-fluid, 2-T MHD including the radiation transfer, with taking into account some model of the small-scale EMHD effects in a rarefied corona of *z* pinch (Kingsep & Rudakov, 1995). For the modeling of the effects of Rayleigh–Taylor instability, we assign small disturbance of the form of free boundary. In the calculations we used a sinusoidal-like perturbation with the amplitude of 0.5–5% from initial *z*-pinch radius.

In Figures 8–10, the far nonlinear stage of the instability has been presented. These results were obtained by A.I. Lobanov's group (Kingsep *et al.*, 1997). One of the most important conclusions derived just from this series of simulations is the following: Even the well-developed Rayleigh–Taylor instability in its nonlinear stage does not violate the efficiency of the longitudinal electron heat transfer, since in some vicinity of the *z*-pinch axis the axial magnetic field B_z continues to dominate. As a whole, simulations confirm the correctness of the liner-converter scheme. However, to realize it, current values more than 10 MA must be achieved.

6. EXPERIMENTS WITH HETEROGENEOUS LINERS

The key point of the liner-converter scheme is the functional separation of the energy carrier and radiator. The electrons of the weakly radiating (e.g., hydrogen) plasma heated due to the magnetic implosion transport their energy onto the highly radiating converter *via* the longitudinal electron heat conductivity. However, contradictory requirements to the plasma parameters necessary for the heat conductivity scheme were implemented, preventing its realization. In fact, at the first stage, energy of the imploding plasma is concentrated in the kinetic energy of the shell. In the next phase, as a result of implosion, it becomes transformed into the ion heat, and then, electrons become heated through Coulomb collisions and adiabatic compression. Estimations show that in low-Z plasmas (H_2, He) the process of the heat transfer from ions to electrons is the slowest stage, limiting the whole efficiency.

Electron heating may be enhanced by choosing higher Z values. This results, however, in a decrease in the heat conductivity. As a consequence, the heat flux cannot provide the transport of the proper energy amount during the time the *z* pinch is being compressed. Besides, *z* pinches or liners pro-

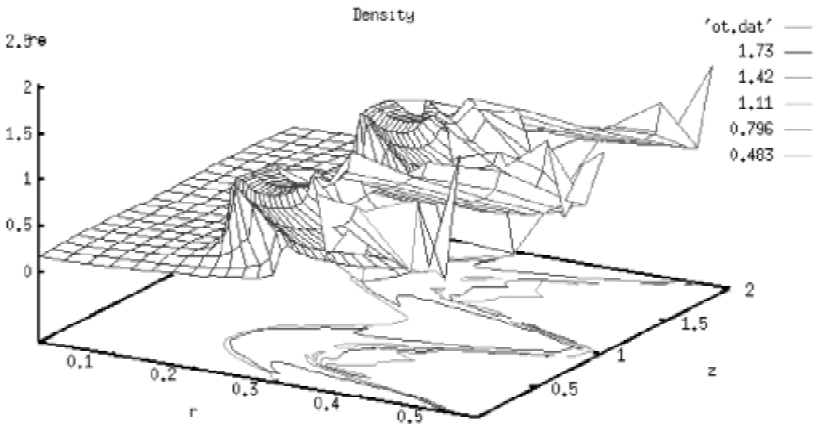

Fig. 8. The calculated density distribution at 92.6 ns. One readily can see mushroom-like structures in the nonlinear stage of Rayleigh–Taylor instability.

https://doi.org/10.1017/S0263034601193110 Published online by Cambridge University Press

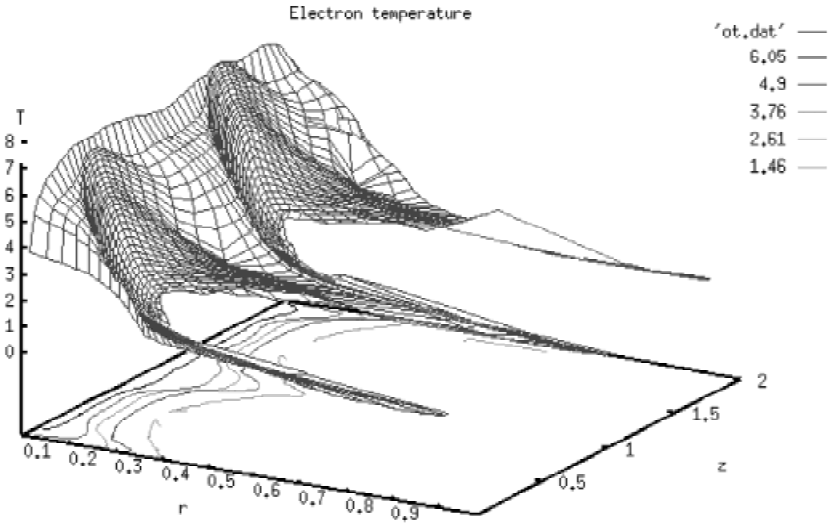

Fig. 9. The calculated electron temperature distribution at 88.2 ns. There is an entropy layer in the vicinity of the axis $r = 0$.

duced from the high-Z plasmas form a very thin current-carrying shell during implosion, which is very unstable (see Sections 3 and 4). The losses due to the soft X-ray radiation increase, too.

These contradictions may be overcome by creating z pinches with complicated structures. To wit, one has to separate in space regions of the efficient electron–ion energetic exchange and regions with high electron heat conductivity. A possible way to do that is a z pinch consisting of two coaxial cylinders. The inner cylinder has to consist of the substance with "intermediate" Z (e.g., Ar) while the outer cylinder has to be produced with low-Z gases (H_2, He). During implosion, the electron–ion energy exchange will occur in the Ar plasma, with the subsequent transport of the electron heat along the outer shell; this electron heat conductivity is much greater. Such a z-pinch configuration has to be more stable due to the absence of the Hall instabilities and the reduction of Rayleigh–Taylor instabilities enhanced by the low-Z values and the large thickness of the plasma shell, respectively.

Taking these considerations into account, we paid special attention to the magnetic compression of the thick He jet in our study of stability of liner implosion (Kingsep & Rudakov, 1995; Bakshaev *et al*., 1998). These experiments were performed on the S-300 installation with the current through the liner load up to 3.5 MA. As a liner, we used cylindrical He jet with outer diameter ~4 cm produced by using a pulse-driven valve and an annular supersonic nozzle. In these experiments, the maximal shell velocity of 5×10^7 cm/s was achieved. For comparison, we carried out also some experiments with the Ar liner having much better radiation ability. In a result of our experiments, two features of the He-liner implosion were observed, namely, the symmetric formation of the shell during compression and good reproducibility of the dynamics. Both can serve as evidence of its stability. In some experiments, we observed an insta-

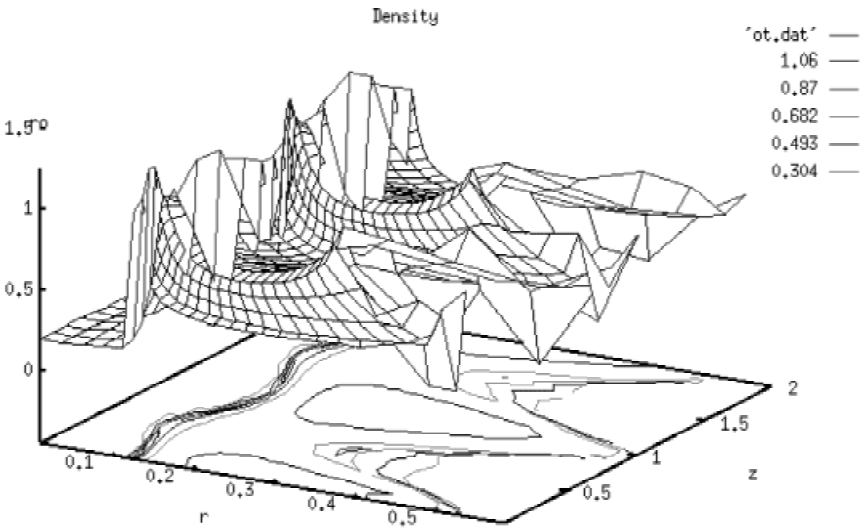

Fig. 10. Dynamics of liner implosion including EMHD effects. At 93.4 ns, the form of Rayleigh–Taylor instability "mushrooms" was transformed, and the liner velocity decreased.

https://doi.org/10.1017/S0263034601193110 Published online by Cambridge University Press

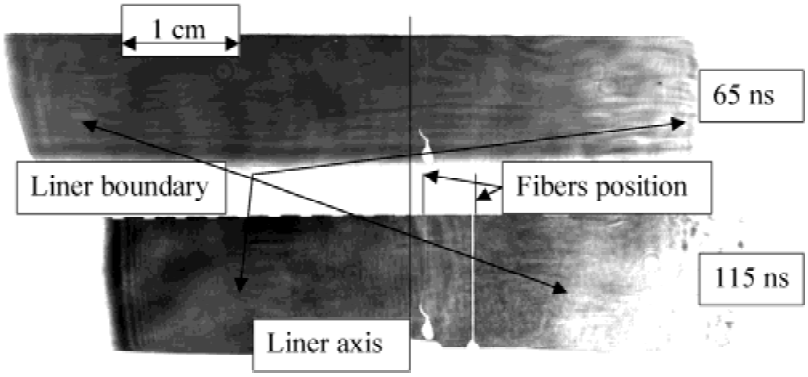

Fig. 11. Glass fibers at the initial position (top) and their explosion after the thermal wave approaches (bottom).

bility of the outer surface of He *z* pinch, before any acceleration. Hence, this instability cannot be related to the Rayleigh–Taylor instability and should be identified as originating from Hall effects. While the implosion of a He liner is "thick," that is, $\delta \sim R$, this instability disappears little by little, without any effect at the final stage of compression. Unlike the He liner, the Ar liner was moving in the "thin" regime, $\delta \ll R$, and manifested some instabilities, starting from the Hall instability resulting in the early stratification, and being completely destroyed at the moment when $R_{outer}/R_{inner} \sim 1/2$.

Our method of heterogeneous pinch creation is based on the production of intermediate-*Z* plasmas by means of evaporation of thin fibers of proper chemical composition situated inside the initial gas jet. These fibers have to be stretched parallel to the axis and form a cylindrical surface of the radius several times less than the initial radius of the gaseous column. Evaporation would be brought about by the front of the heat wave, which, in turn, would be generated in the light gas by the shock wave resulting from the magnetic piston. Some preliminary estimates show that with taking the fibers as thin as 1–3 μm, one obtains a plasma expansion of about 1–2 mm during a time ~10 ns. Thus, by placing the fibers in an array dense enough, one can produce a continuous plasma cylinder with the necessary Z_{eff}. It is important to note that such a manner of plasma formation is free from instabilities accompanying the current flow, as well as the possible gases mixing during the heterogeneous gaseous structure creation.

Plasma, with moderately high *Z* value, was produced by evaporation of thin glass fibers when they were approached by the temperature wave from the He plasma (Fig. 11). Initially these fibers were disposed along the circumference near the liner axis. By means of Schlieren photography and shadowgraphy we may identify the fiber explosion at the moment of time when the thermal wave initiated by *z*-pinch compression reaches the radius where the fibers are situated. In principle, such an explosion could be provoked by the magnetic precursors. We can differentiate, however, between the current-driven fiber explosion scenario and the explosion that we could observe. The latter may be characterized by the smooth profile of the "glass plasma" surface, unlike the well-known "fractal" structure resulting from the current-driven blow-up.

The effect of adding the impurities with higher *Z* value on the heating of electrons and on the heat conductivity was determined by registration of spectral lines of the He-like chlorine ions placed at the cathode end of liner gap as a thin layer of pure NaCl. The X-ray spectra reveal a series of lines of H- and He-like ions of the elements being components of the glass (Al, Si, Ca, and others) with the excitation energies up to 4 keV (Fig. 12). One can see here the resonant line of the He-like chlorine looking like the 3-mm-sized bright spot on the cathode. In the absence of fibers, the intensity of this line is less by at least several times, which is evidence of increasing the heat conductivity in the presence of the higher-*Z* impurities.

7. CONCLUSIONS

The stability of the fast hollow *z* pinch (light liner) was studied on Module A-5 and S-300 installations. A new class of fast, EMHD (Hall) instabilities was observed. The stabilization of light liners by means of an external longitudinal magnetic field has been demonstrated in the experiment.

First the "snow-plough" regime was observed in the experiments on the Module A-5 machine. Analytical theory has been developed which predicts the overheating instability of the current-carrying shell resulting in formation of a very thin, light, and hot current sheath. It may result, in turn, in the inner breakdown, formation of magnetic precursors, and small-scale Rayleigh–Taylor instability.

On the basis of a heterogeneous *z* pinch, an enhanced efficiency of ion–electron energy exchange has been achieved, resulting in the enhanced heat flux onto the edge converter.

ACKNOWLEDGMENTS

The work was partially supported by the joint European INTAS grant 97-0021 and Russian Foundation for Basic Research, grant 98-02-17616.

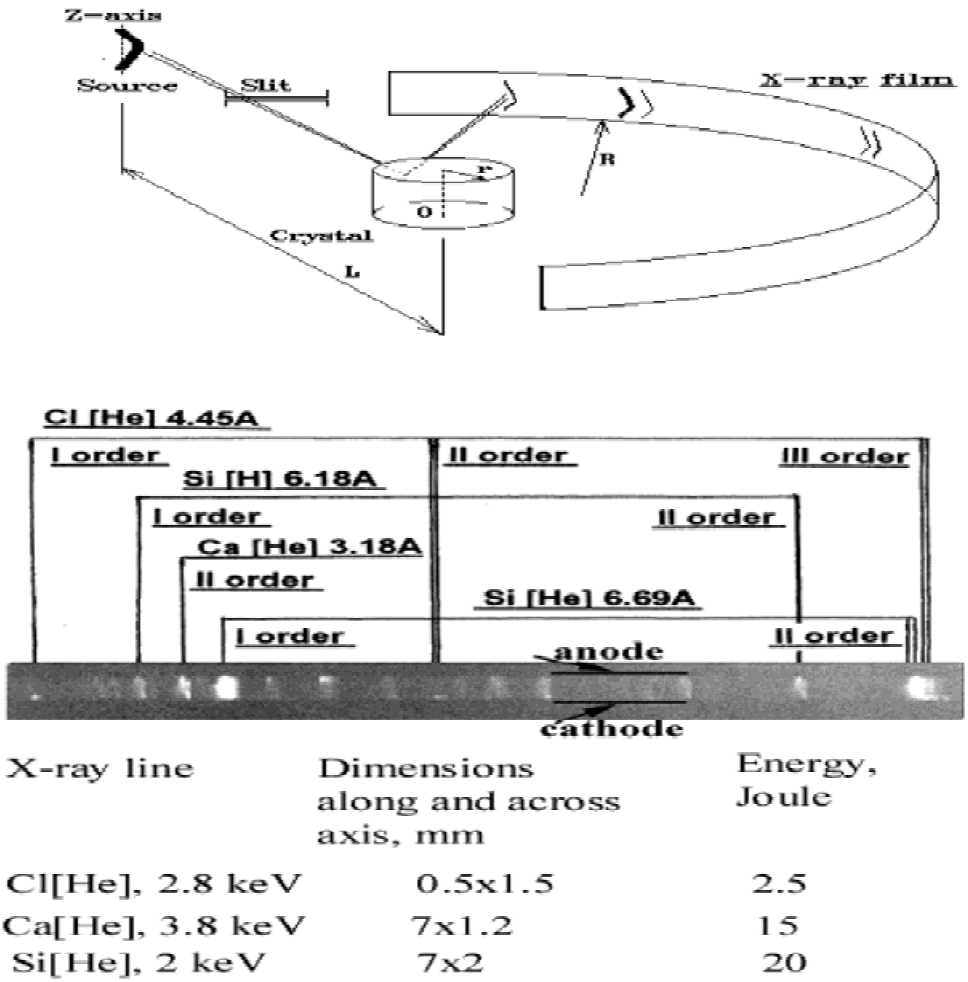

X-ray line	Dimensions along and across axis, mm	Energy, Joule
Cl[He], 2.8 keV	0.5x1.5	2.5
Ca[He], 3.8 keV	7x1.2	15
Si[He], 2 keV	7x2	20

Fig. 12. Mica spectrograph (top) and lines of H- and He-like ions observed (bottom).

REFERENCES

Bakshaev, Yu.L. *et al.* (1997). *Proc. Eighteenth Symp. on Plasma Phys. and Technol.*, Prague, p. 45.

Bakshaev, Yu.L. *et al.* (1998). *Proc. Twelfth Int. Conf. on High Power Beams*, Haifa, p. 244.

Baranchikov, E.I. *et al.* (1978). *Sov. Physics JETP* **75**, 2101.

Bogolyubsky, S.L. *et al.* (1988). *Proc. Seventh Int. Conf. on High Power Beams*, Karlsruhe, p. 1255.

Bol'shakov, V.P. *et al.* (1982). *Atomnaya Energiya (Atomic Energy)* **53**, 14.

Braginskii, S.I. (1963). *Reviews of Plasma Physics* (Leontovich M.A., Ed.), Vol. 1. New York: Consultants Bureau.

Chernenko, A.S. *et al.* (1996). *Proc. Eleventh Int. Conf. on High Power Beams*, Prague, Vol. 1, p. 154.

Chukbar, K.V. (1993). *Plasma Phys. Reports* **19**, 783.

Gasque, A.-M. *et al.* (1998). *Plasma Phys. Reports* **24**, 672.

Grigor'ev, S.F. & Zakharov, S.V. (1987). *Sov. Tech. Phys. Lett.* **13**, 254.

Kingsep, A. *et al.* (1999). *Proc. First Int. Conf. on Inertial Fusion Science and Applications*, Bordeaux, MO1c5, Report 141.

Kingsep, A.S. & Rudakov, L.I. (1995). *Plasma Phys. Reports* **21**, 611.

Kingsep, A.S. *et al.* (1990). *Rev. of Plasma Physics* (Kadomtsev, B.B., Ed.), Vol. 16. New York: Consultants Bureau.

Kingsep, A.S. *et al.* (1997). *Plasma Phys. Reports*, **23**, 879.

Kosarev, V.I. *et al.* (1989). *Topics in Atomic Science and Technology*, Vol. 13. Moscow: Gosatomizdat.

Neudachin, V.V. & Sasorov, P.V. (1991). *Nucl. Fusion* **31**, 1053.

Quintenz, J.P. *et al.* (2000). *Proc. Thirteenth Int. Conf. on High Power Beams*, Nagaoka.

Rudakov L.I. (1989). *Proc. Second Int. Conf. on Dense Z-Pinches*, Laguna Beach, p. 290.

Rudakov, L.I. & Sevastianov, A.A. (1996). *Proc. Eleventh Int. Conf. on High Power Beams*, Prague, Vol. 2, p. 776.

Rudakov, L.I. *et al.* (1990). *Proc. Seventeenth European Conf. on Controlled Fusion and Plasma Physics*, Amsterdam, Vol. 2, p. 609.

Rudakov, L.I. *et al.* (1991). *Phys. Fluids B* **3**, 2414.

Rudakov, L.I. *et al.* (1997). *Proc. Fourth Int. Conf. on Dense Z-Pinches*, Vancouver, p. 187.

Sasorov, P.V. (1991). *Sov. J. Plasma Phys.* **17**, 874.

Zehnter, P. *et al.* (1998). *Proc. Int. Congress on Plasma Physics*, Prague, F090, p. 1666.

https://doi.org/10.1017/S0263034601193110 Published online by Cambridge University Press